JPET Fast Forward. Published on October 8, 2024 as DOI: 10.1124/jpet.124.002424
This article has not been copyedited and formatted. The final version may differ from this version.

Metformin in Overcoming Enzalutamide Resistance in Castration-Resistant Prostate Cancer

Kendall Simpson[1], Derek B. Allison[2,3], Daheng He[3], Jinpeng Liu[3,4], Chi Wang[3,4], and Xiaoqi Liu[1,4,*]

[1] Department of Toxicology and Cancer Biology, University of Kentucky, Lexington, Kentucky 40536, USA

[2] Department of Pathology & Laboratory Medicine, University of Kentucky, Lexington, Kentucky 40508, USA

[3] Markey Cancer Center, University of Kentucky, Lexington, Kentucky 40536, USA

[4] Department of Internal Medicine, University of Kentucky, Lexington, Kentucky, 40536, USA

JPET Fast Forward. Published on October 8, 2024 as DOI: 10.1124/jpet.124.002424
This article has not been copyedited and formatted. The final version may differ from this version.

Running title: Metformin in enzalutamide resistance

* Corresponding Author: Xiaoqi Liu, University of Kentucky, HKRB, Rm 352, 760 Press Avenue, Lexington, KY 40536. Phone: 859-257-3760; Fax: 859-323-1059; E-mail: xiaoqi.Liu@uky.edu

Number of text pages: 25
Number of tables: 0
Number of figures: 5
Number of references: 42
Number of words in Abstract: 210
Number of words in Introduction: 515
Number of words in Discussion: 1488

ABBREVIATIONS:

ADT, androgen depravation therapy; AR, androgen receptor; CDKs, cyclin-dependent kinases; CRPC, castration-resistant prostate cancer; DMSO, dimethyl sulfoxide; ECAR, extracellular acidification rate; ENZ-r, Enzalutamide-resistance; ETC, electron transport chain; FCCP, carbonyl cyanide-p-trifluoromethoxyphenylhydrazone**;** H&E, hematoxylin and eosin; HSA, highest single agent; IC_{50}, half-maximal inhibitory concentration; IHC, immunohistochemistry; JC-1, 5,5',6,6'-Tetrachloro-1,1',3,3'-tetraethylbenzimidazolylcarbocyanine iodide; MMP, mitochondrial membrane potential; NSG, NOD scid gamma; OCR, oxygen consumption rate; OXPHOS, oxidative phosphorylation; PARP, poly(ADP-ribose) polymerase; PCa, prostate cancer; Plk1, polo-like kinase 1; TMRE, tetramethylrhodamine ethyl ester

Recommended Section assignment: Drug Discovery and Translational Medicine

JPET Fast Forward. Published on October 8, 2024 as DOI: 10.1124/jpet.124.002424
This article has not been copyedited and formatted. The final version may differ from this version.

Abstract

Androgen deprivation is the standard treatment for prostate cancer (PCa) patients. However, the disease eventually progresses as castration-resistant PCa (CRPC). Enzalutamide, an AR inhibitor, is a typical drug to treating CRPC and due to continuous reliance on the drug, can lead to Enzalutamide-resistance (ENZ-r). This highlights the necessity for developing novel therapeutic targets to combat the gain of resistance. Metformin has been recently investigated for its potential anti-tumorigenic effects in many cancer types. In this study, we used enzalutamide and metformin in combination to explore the possible rescued efficacy of enzalutamide in the treatment of ENZ-r CRPC. We first tested the effects of this combination treatment on cell viability, drug synergy, and cell proliferation in ENZ-r CRPC cell lines. After combination treatment, we observed a decrease in cell proliferation and viability as well as a synergistic effect of both enzalutamide and metformin *in vitro*. Following these results, we sought to explore how combination treatment effected mitochondrial fitness utilizing mitochondrial stress test analysis and mitochondrial membrane potential (MMP) shifts due to metformin's action in inhibiting Complex I of oxidative phosphorylation. We employed 2 different strategies of *in vivo* testing using 22Rv1 and LuCaP35CR xenograft models. Finally, RNA sequencing revealed a potential link in the downregulation of Ras/MAPK signaling following combination treatment.

Significance Statement

Increasing evidence suggests that oxidative phosphorylation might play a critical role in the development of resistance to cancer therapy. We showed that targeting oxidative phosphorylation with metformin can enhance the efficacy of enzalutamide in castration-resistant prostate cancer in vitro.

JPET Fast Forward. Published on October 8, 2024 as DOI: 10.1124/jpet.124.002424
This article has not been copyedited and formatted. The final version may differ from this version.

Introduction:

Prostate cancer (PCa) has the highest number of new cases in men in the United States with approximately 299,010 new cases in 2024 and is the second leading cause of cancer related deaths with an estimated 35,250 deaths in 2024 (Siegel et al., 2024). Early stage PCa patients that undergo localized therapies, radial prostatectomy, and hormone therapies will often experience cancer regression and symptom relief (Shoag et al., 2020). Hormone therapy, commonly referred to as androgen depravation therapy (ADT), is utilized to prevent androgen receptor (AR) signaling and therefore PCa progression, however, over time many patients will often experience recurrence and are considered to have castration-resistant prostate cancer (CRPC) (Chandrasekar et al., 2015; Sharifi et al., 2005). Upon cancer recurrence, therapeutic options become more limited, and patients will often be treated with FDA-approved AR inhibitors such as abiraterone, enzalutamide, and darolutamide. In the case with metastatic CRPC, the only FDA-approved AR inhibitor available is enzalutamide, however, most patients being treated with enzalutamide over time will experience enzalutamide resistance (Antonarakis et al., 2014; Efstathiou et al., 2015; van Soest et al., 2015). This evidence demonstrates the critical need for the development of novel treatment strategies in advanced drug resistant CRPC.

In recent years, metformin, the most commonly prescribed oral biguanide to treat type II diabetes, has gained traction with its implications in reduced cancer risk and potential utilization as cancer treatments (Kasznicki et al., 2014; Zhao et al., 2019). Metformin has limited side effects and an excellent safety profile so investigation into possible drug-repurposing as a cancer therapy is an attractive option in many cancer types (Sleire et al., 2017). In addition to numerous mechanistic studies in PCa utilizing metformin as a cancer therapy (Ben Sahra et al., 2008; Chen et al., 2016; Kong et al., 2020; Shao et al., 2015), there have been multiple clinical trials in recent

JPET Fast Forward. Published on October 8, 2024 as DOI: 10.1124/jpet.124.002424
This article has not been copyedited and formatted. The final version may differ from this version.

years exploring this mechanism of cancer treatment (Murtola et al., 2008; Spratt et al., 2013). In particular, a phase II clinical trial in Switzerland utilized combination treatment of enzalutamide and metformin in CRPC patients who have never been exposed to enzalutamide and other endocrine agents (Rothermundt et al., 2014). While there is validity in utilizing enzalutamide and metformin in combination for CRPC patients, there is little known about this combination treatment in drug-resistant CRPC.

In this study, we found that combination treatment of enzalutamide and metformin in established drug-resistant CRPC lines demonstrate a synergistic anti-proliferative effect *in vitro*. In addition, we investigated the effect of combination treatment on mitochondrial function utilizing a mitochondrial stress test seahorse assay and measuring the mitochondrial membrane potential (MMP), however, we did not observe any significant effects on drug-resistant CRPC lines. To validate our synergy results *in vivo*, we employed two different xenograft models to determine the effects of combination treatment on tumor growth, however, we did not observe a difference in tumor growth between treatment groups. Finally, we treated drug-resistant CRPC lines with combination therapies for RNA sequencing to determine a mechanistic link. Together, these results highlight the importance of utilizing robust models in cancer research to test novel treatment strategies.

Materials and Methods:

Cell Culture, Chemicals, and Reagents

LNCaP, MR49F, C4-2, C4-2R, and 22Rv1 cell lines were used in this study. LNCaP cells are androgen-dependent cells, however, C4-2 cells were derived from LNCaP cells and are androgen independent. In a similar fashion, MR49F cells are also derived from LNCaP cells, however, MR49F cells are enzalutamide resistant. C4-2R cells are enzalutamide resistant cells derived from

JPET Fast Forward. Published on October 8, 2024 as DOI: 10.1124/jpet.124.002424
This article has not been copyedited and formatted. The final version may differ from this version.

C4-2 cells. C4-2 cells were obtained from the M. D. Anderson Cancer Center whereas MR49F and C4-2R cells were kindly provided by Dr. Amina Zoubeidi at the Vancouver Prostate Cancer Center and Dr. Allen Gao at University of California at Davis, respectively. LNCaP and 22Rv1 cells were purchased from ATCC. All cells were cultured in RMPI-1640 media supplemented with 10% (v/v) fetal bovine serum, 100 units/mL penicillin, and 100units/mL streptomycin incubated at 37°C and 5% CO2. MR49F and C4-2R were maintained in 10μM and 20μM enzalutamide solution, respectively to maintain resistance. Enzalutamide was purchased from MedChemExpress (HY-70002). Metformin HCl, Onvansertib [NMS-P937], and Carbonyl cyanide-4-(trifluoromethoxy) phenylhy-drazone (FCCP) were purchased from Selleckchem (S1950, S7255, S8276).

Clonogenic Assay

MR49F, C4-2R, and 22Rv1 cells were seeded (3-6X10^3/well) into 6-well plates with 3mL of RPMI-1640. The following day, cells were treated with varying drugs as indicated and incubated at 37°C. Cells were treated every other day for 10 days, then washed with ice cold 1X PBS, fixed with ice cold methanol for 10 minutes on ice, and stained with 0.5% crystal violet staining solution. Relative well intensity was calculated using ImageJ software.

Cell Viability and Synergy

MR49F, C4-2R, and 22Rv1 cells were seeded (6x10^3/well) into 96-well plates with 100μL of RMPI-1640. 24 hours later, cells were treated with varying drugs at the indicated concentrations and allowed to incubate for 72 hours. To assess cell viability, AquaBluer solution (also known as Alamar Blue) was added to each well in a 1:100 ratio of AquaBluer solution: culture media, which monitors the reducing environment of the living cell. Cells were incubated for 4 hours at 37°C before measuring the fluorescent intensity 540ex/590em via GloMax Discover microplate reader (Promega). Cells were seeded in quadruplicate for each drug concentration and the readings were

JPET Fast Forward. Published on October 8, 2024 as DOI: 10.1124/jpet.124.002424
This article has not been copyedited and formatted. The final version may differ from this version.

all normalized to average blank control wells without cells. The results are expressed as the percentage of viable cells with respect to the negative control (dimethyl sulfoxide, DMSO) which represents 100% viability shown above. Synergy scores were calculated using SynergyFinder.org.

Protein Immunoblotting

Cells were previously treated with varying drug combinations for 48 hours before harvest. Cell lysis was achieved by 10% RIPA solution with protease and phosphatase inhibitors followed by sonication. Protein concentration was measured by Pierce BCA Assay kit and equal concentrations of protein lysate from each sample were mixed with SDS loading buffer, resolved on an SDS-Page gel electrophoresis, and transferred to either Nitrocellulose or PVDF membranes followed by blocking and incubation with primary and HRP-conjugated secondary antibodies. ECL was used to induce chemiluminescence and membranes were imaged using BioRad ChemiDoc MP. BioRad ImageLab software was utilized to analyze immunoblots.

Seahorse Analysis

MR49F, C4-2R, and 22Rv1 cells were seeded ($2x10^4$/well) into XFe96 cell culture microplates in RPMI-1640 culture medium and incubated for 24 hours. Cells were then treated with varying drug concentrations as indicated for 24 hours prior to analysis. Both the oxygen consumption rate (OCR) and the extracellular acidification rate (ECAR) were measured using the seahorse XFe96 analyzer from Agilent. Mitochondrial stress test was performed by first measuring the initial OCR rate for cells, followed by 1μM oligomycin which inhibits complex V of oxidative phosphorylation (OXPHOS) (indicative of the ATP production rate). Next, 1-2μM of FCCP treatment was used to uncouple the proton gradient and determine maximum respiration (FCCP titration experiment to determine optimal FCCP dose was conducted prior to analysis). Following this, 1μM of both rotenone and antimycin A were given, which inhibits complexes I and III, respectively.

JPET Fast Forward. Published on October 8, 2024 as DOI: 10.1124/jpet.124.002424
This article has not been copyedited and formatted. The final version may differ from this version.

Flow Cytometric Analysis

For measuring MMP, cells were seeded (between $5x10^5$ and $1x10^6$/well) into 6 well plates with 3 mL of RPMI-1640 per and allowed to incubate for 24 hours at 37°C. Cells were treated with various drugs as indicated with an incubation time of 24 hours. 48 hours after initial seeding, cells were trypsinized, collected, and counted for a density of approximately $1x10^6$/mL per sample. FCCP was used as a positive control (20μM) and incubated for 15 minutes at 37°C prior to staining. All samples were then stained at 200nM per sample with either tetramethylrhodamine ethyl ester (TMRE) reagent (Cayman chemical # 701310) or 5,5',6,6'-tetrachloro-1,1',3,3'-tetraethylbenzimidazolylcarbocyanine iodide (JC-1) reagent (MedChemExpress # HY-15534) and incubated at 37°C for 30 minutes. Cells were centrifuged at 2,000rpm for 3 minutes and resuspended in 300μL fresh 1xPBS for analysis. Samples were analyzed using BD FACSymphony A5 Cell analyzer and FlowJo software.

RNA Sequencing Analysis

LNCaP, MR49F, C4-2, and C4-2R cells were previously treated with varying drug combinations for 48 hours prior to total RNA extraction. Extraction was achieved using Qiagen's RNeasy Mini Kit (#74104) according to the manufacturer's instructions. All samples were sent to Novogene Biotechnology Company (CA, USA) for RNA quality assessment, library construction, Illumina sequencing, and data analysis. DEseq2 R package was used to analyze gene expression data normalization and differential expression. Significantly up/down regulated genes were determined as a fold change of ≥ 2 and q value of <0.05.

22Rv1-derived Xenograft Mouse Model

All animal experiments were approved by the Institutional Animal Care and Use Committee (IACUC) at the University of Kentucky. 22Rv1 cells were mixed with equal volume of Matrigel and inoculated subcutaneously at $2.5x10^6$ cells/mouse into the right flank of pre-castrated nude

JPET Fast Forward. Published on October 8, 2024 as DOI: 10.1124/jpet.124.002424
This article has not been copyedited and formatted. The final version may differ from this version.

mice. After a week following inoculation, mice were randomized into four treatment groups. Treatments were started when the size of tumors reached 200 mm^3. Enzalutamide (30mg/kg) was dissolved in 10% DMSO and 90% corn oil and Metformin HCl (20mg/kg) was dissolved in sterile water and administered through oral gavage daily for 4 weeks (Farah et al., 2022; Kong et al., 2020; Li et al., 2022; Liu et al., 2023; Shao et al., 2015). Tumors were measured every 3 days and tumor volume was estimated using the following formula $V = L\,X\,W^2/2$ where V is volume in cubic millimeters, L is length in millimeters, and W is for width in millimeters.

LuCaP35CR Xenograft Mouse Model

NOD scid gamma (NSG) mice bearing LuCaP35CR tumors were obtained by Dr. Robert Vessella at the University of Washington. For tumor amplification, tumor sections were harvested and implanted subcutaneously into the flanks of pre-castrated NSG mice. When tumors reached a large size, tumors were harvested and sectioned into approximately 25mm^3 pieces. Tumor pieces were implanted into 40 pre-castrated NSG mice. Once the tumors reached approximately 200mm^3, mice were randomized into 4 treatment groups. Enzalutamide (30mg/kg) was dissolved in 10% DMSO and 90% corn oil and metformin HCl (20mg/kg) was dissolved in sterile water and administered through oral gavage daily for 4 weeks. Tumors were measured every 3 days and tumor volume was estimated using the following formula $V = L\,X\,W^2/2$ where V is volume in cubic millimeters, L is length in millimeters, and W is for width in millimeters.

Histology and Immunohistochemistry

Xenograft tumors were fixed in 10% neutral-buffered formalin with rocking overnight and transferred into 70% ethanol the following day. Tumors were paraffin embedded, sectioned to 5mM sections, mounted, and processed using conventional hematoxylin and eosin (H&E) staining. Sections were also stained for the Ki67 proliferation marker and cleaved caspase 3.

JPET Fast Forward. Published on October 8, 2024 as DOI: 10.1124/jpet.124.002424
This article has not been copyedited and formatted. The final version may differ from this version.

Statistical Analysis

Numerical data is represented as mean ± SD. Statistical significance of the results was analyzed by using unpaired two-tailed t test. The p values of <0.05 indicates statistical significance.

Results:

Metformin treatment exhibits a synergistic effect with enzalutamide in ENZ-r CRPC lines.

To determine the optimal doses of either enzalutamide or metformin for the attenuation of prostate cancer growth *in vitro*, we first utilized a cell viability assay and calculated IC_{50} values. For both isogenic lines, the enzalutamide sensitive IC_{50}s of enzalutamide were lower than their enzalutamide resistant counterparts where LNCaP and C4-2 IC_{50} values were 14.5μM and 22μM respectively, MR49F and C4-2R IC50 values were 26μM and 35μM respectively (**Fig 1A,C**) which were consistent with our previous findings (Bai et al., 2019). The IC_{50} value for enzalutamide-resistant 22Rv1 cells was 110μM (**Fig 1E**). The same strategy was applied to measure the IC_{50} values of metformin where LNCaP was 2.1mM, MR49F was 3.2mM, C4-2 was 4.1mM, C4-2R was 1.7mM, and 22Rv1 was 15.4mM (**Fig 1B,D,F**). Utilizing these doses, we sought to test whether metformin would enhance enzalutamide inhibition of cell growth using a clonogenic assay. All three ENZ-r lines were seeded at a low density and treated with DMSO as a control, 10μM, 20μM, or 30μM of enzalutamide for MR49F, C4-2R, or 22Rv1 respectively, 1mM of metformin alone or in combination with enzalutamide for 14 days followed by crystal violet stain (**Fig 1G-I**). From the quantification, all three ENZ-r lines exhibited varying decreases in cell growth in mono treatment. However, combination treatment exhibited the greatest significant cell growth attenuation ($p \leq 0.001$). To test whether metformin synergizes with enzalutamide to inhibit cell proliferation, we utilized a cell viability assay. Cells were treated with increasing combinations of enzalutamide or metformin and analyzed using the highest single agent (HSA) synergy model.

JPET Fast Forward. Published on October 8, 2024 as DOI: 10.1124/jpet.124.002424
This article has not been copyedited and formatted. The final version may differ from this version.

We observed a strong synergistic effect in ENZ-r cells treated with a minimum of 1mM metformin in combination with enzalutamide (**Fig 1J-L**). Together, these results suggest that enzalutamide and metformin have a synergistic effect on drug resistant prostate cancer growth *in vitro*.

Combination treatment results in metabolic reprogramming

Previous studies demonstrated the reliance of OXPHOS in advanced PCa (Cutruzzola et al., 2017). We hypothesized that utilizing metformin in combination with enzalutamide would subject the PCa cells to an energy crisis and vulnerability to apoptosis. To gain a better understanding of the effect of combination treatment on mitochondrial function, we treated ENZ-r cells followed by a mitochondrial stress test via seahorse analysis. We utilized the mitochondrial stress test to directly measure OCR of cells following injection of key modulators of cellular respiration to determine mitochondrial function (Ferrick et al., 2008; Horan et al., 2012). In MR49F cells, combination treatment lowered basal respiration, proton leak, ATP production, and spare respiratory capacity indicating an overall decline OXPHOS (**Fig 2A-C**). Similarly, we confirmed these findings in C4-2R cells where the basal respiration, proton leak, and ATP production was decreased compared to control cells, however, C4-2R cells were markedly more sensitive to metformin treatment as the overall OCR was much lower compared to MR49F (**Fig 2D-F**). Interestingly, combination treated C4-2R cells exhibited a higher spare respiratory capacity than metformin treatment alone indicating an increased capability of the cell to respond to energetic demand. Next, we sought to measure the MMP in response to combination treatment as an indicator of ATP production (Sukumar et al., 2016). As the MMP depolarizes, the membrane will become more permeable allowing protons to diffuse out of the intermembrane space. Disruption of the proton gradient will inhibit ATP synthase resulting in an overall inhibition of OXPHOS. We utilized TMRE, a fluorescent chemical indicating metabolic fitness, to stain ENZ-r cells following combination treatment followed by flow cytometric analysis. FCCP, an electron transport chain (ETC)

JPET Fast Forward. Published on October 8, 2024 as DOI: 10.1124/jpet.124.002424
This article has not been copyedited and formatted. The final version may differ from this version.

uncoupler, was used as a positive control for near complete depolarization of the MMP. All samples were normalized to FCCP where TMRE-positive cells are indicative of MMP depolarization. In both MR49F and 22Rv1 cells, we did not observe any difference in MMP depolarization 24 hours after treatment (**Fig 2G, I**). Interestingly, we observed an increase in TMRE fluorescence in combination treatment compared to control which indicates an overall increased metabolic fitness (**Fig 2H**). These data are consistent with our results from the mitochondrial stress test, in that C4-2R cells seem to exhibit increased mitochondrial function in response to combination treatment. Finally, to confirm our results from TMRE, we employed a similar method of measuring MMP with the JC-1 chemical which is considered more sensitive than TMRE. JC-1 differs from TMRE in that upon entrance into the mitochondria, the aggregate will emit a red color, indicative of a polarizes and metabolically energetic MMP. Following depolarization of the MMP, JC-1 will present as monomers and diffuse out of the intermembrane space, emitting a green color. After flow cytometric analysis, we observed a similar ratio of red/green % cells between control, enzalutamide and combination in MR49F cells with metformin solo treatment having the greatest effect at depolarization of the MMP (**Fig 2J**). In C4-2R cells, metformin mono treatment and combination treatment remain similar to control in MMP. Due to the large error bar of the C4-2R enzalutamide mono treatment, further replicates need to be performed to generate conclusive data. 22Rv1 cells exhibited a similar effect on MMP across all treatment groups. Together, this data suggests that combination treatment may have a small effect on metabolic fitness of the mitochondria, however, conclusive evidence is lacking at this time.

Combination treatment effect on 22Rv1-derived xenograft tumors

To investigate our findings in vitro, we evaluated the effect of enzalutamide and metformin alone or in combination with a 22Rv1-derived xenograft mouse model. 22Rv1 cells express the

JPET Fast Forward. Published on October 8, 2024 as DOI: 10.1124/jpet.124.002424
This article has not been copyedited and formatted. The final version may differ from this version.

AR-V7 splice variant of AR which harbors a truncated form of the ligand binding domain and preventing enzalutamide binding, making these cells intrinsically resistant to enzalutamide (Sobhani et al., 2021). Following 50 days of treatment, metformin alone exhibited a similar rate of tumor growth as control while enzalutamide alone and combination treatment groups had similar rates to each other (**Fig 3A**). Similarly, the tumor weights for all 3 treatment groups after harvest were not significantly decreased compared to control (**Fig 3B**). Images from the harvested tumors confirm our results ultimately observing no significant changes in tumor size compared between groups (**Fig 3C**). There was no observable difference in body weight between groups indicating a lack of treatment toxicity (**Fig 3D**). Following harvest, we processed the tumors for IHC analysis. H&E staining of tumor samples did not show any significant difference among different groups (**Fig 3E**). To measure proliferation, we stained IHC samples with proliferation marker Ki67 and observed what appears to be a general decrease in proliferation in combination treated tumors, however, further analysis and confirmation by a pathologist would be required to make such claim (**Fig 3F**). Finally, cleaved caspase-3 staining of tumor samples indicated a similar level of apoptosis across samples, although further studies will be required to confirm these results (**Fig 3G**). Interestingly, despite observation of an inhibition of PCa cell growth *in vitro*, we did not observe the same effects on PCa growth *in vivo* following combination treatment.

Combination treatment effect on LuCaP35CR xenograft tumors

To further investigate the results of our *in vitro* work, we also employed a LuCaP35CR xenograft model, which is more closely related to patient samples, to determine the effect of combination treatment on tumor growth. Consistent with our previous results in the 22Rv1-derived xenograft experiment, LuCaP35CR did not exhibit any significant changes in tumor volume within the 4 treatment groups 50 days following initial treatment (**Fig 4A**). Immediately upon harvest

JPET Fast Forward. Published on October 8, 2024 as DOI: 10.1124/jpet.124.002424
This article has not been copyedited and formatted. The final version may differ from this version.

tumors were weighed and exhibited no significant changes between treatment group tumors (**Fig 4B**) or between tumor size indicated by the tumor images in **Figure 4C**. To determine toxicity, we measured body weight in the 4 groups throughout the study and while there may be an observable difference between treatment groups and control, this could be due to the small sample size for all groups (n=5) (**Fig 4D**). Taken together, our *in vivo* results indicate a lack of synergistic effect *in vivo*, in contrast to the phenotype we observed *in vitro*.

RNA Sequencing analysis of isogenic ENZ-r CRPC lines.

To determine the mechanism in which CRPC lines respond to combination treatment, we performed RNA sequencing analysis with the isogenic sensitive and ENZ-r lines listed previously. After enzalutamide or metformin mono treatment or in combination, we compared gene lists to determine differences in RNA expression in for genes that were specific to ENZ-r combination treated samples (**Fig 5A**). C4-2R combination treated gene sets exhibit a significant decrease in genes in the Ras signaling pathway as well as phospholipase D signaling and genes related to the lipid and atherosclerosis pathway (**Fig 5B**). Based on these results, we can speculate that a downregulation in Ras signaling specifically would inhibit cell growth and proliferation (Weber and Gioeli, 2004). In addition, phospholipase D signaling as well as lipid and atherosclerosis signaling play roles in cellular metabolism as well as cross signaling with traditional oncogenic signaling pathways such as Ras, mTOR, and MAPK signaling, and we observe their downregulation in our samples (Edlind and Hsieh, 2014; Rodriguez-Berriguete et al., 2012; Shorning et al., 2020; Weber and Gioeli, 2004). We observed similar results in the significant down regulation of genes associated with the MAPK signaling, lipid and atherosclerosis pathways and calcium signaling. As with C4-2R cells, these down regulated pathways foreshadow a shift in gene expression towards the inhibition of cell proliferation and cellular metabolism pathways (**Fig 5D**). In contrast, we observe an up-regulation of both cell cycle signaling proteins as well as proteins

JPET Fast Forward. Published on October 8, 2024 as DOI: 10.1124/jpet.124.002424
This article has not been copyedited and formatted. The final version may differ from this version.

related to various DNA repair pathways in both C4-2R (**Fig 5C**) and MR49F (**Fig 5E**) following combination treatment. It is currently unclear how the upregulation of these genes may influence these ENZ-r prostate cancer cells; further analysis is required to investigate these results.

Discussion

While treatments and therapies continue in development for various cancers at different stages, drug resistance remains a serious issue in advanced CRPC and identifying novel treatment strategies is critical (Amaral et al., 2012; Seruga et al., 2011). Enzalutamide, as a competitive inhibitor of AR signaling, continues to be the only FDA-approved therapy for metastatic CRPC, however, resistance to treatment often occurs. In this study, we assessed whether combination treatment of enzalutamide and metformin in enzalutamide-resistant PCa lines would induce an energy crisis and therefore induce vulnerability to apoptosis (Wang et al., 2021). Our results demonstrate that the combination treatment is synergistically compatible to inhibit drug resistant PCa growth *in vitro*. Cell proliferation in ENZ-r was significantly inhibited following combination treatment (**Fig. 1G-I**) and our results indicate that the two drugs tested act synergistically together using an HSA synergy model (**Fig. 1J-L**) (Berenbaum, 1989). These results suggest a vulnerability in the metabolic signaling of ENZ-r PCa cells which may have allowed for exploitation and ultimately cell death with enzalutamide treatment.

While our combination treatment exhibited a similar growth inhibition phenotype across all 3 ENZ-r lines, we observed differences in mitochondrial function between these lines. It has been well documented that the mitochondrial stress test is a robust method in testing mitochondrial function (Ferrick et al., 2008). After combination treatment, MR49F cells exhibited more of a lack in mitochondrial function indicated by an overall lower basal consumption rate, lower spare respiratory capacity, and decreased ATP production (**Fig. 2A-C**). In contrast, combination-treated

JPET Fast Forward. Published on October 8, 2024 as DOI: 10.1124/jpet.124.002424
This article has not been copyedited and formatted. The final version may differ from this version.

C4-2R cells responded similarly to metformin mono treatment with a decreased basal respiration rate and ATP production, however, combination treatment may have a better capacity to respond to metabolic stress indicated by a higher respiratory capacity (**Fig. 2D-F**). The observed difference in mitochondrial respiration between these two cell lines may be a result of the differences in metabolic gene expression. In addition, utilizing an acute injection mitochondrial stress test and measuring the changes in OCR immediately following treatment may yield interesting changes in respiration as this experiment would capture the immediate responses to treatment. The MMP is maintained by the ETC as a means of producing a proton gradient for ATP synthase to function, therefore, depolarization of the MMP is indicative of OXPHOS inhibition (Sukumar et al., 2016). While we tested two different means in which the MMP can be measured for all 3 ENZ-r lines, we did not observe a significant difference in polarization between treatment groups compared to control (**Fig. 2G-J**). While the MMP is indicative of OXPHOS inhibition, the MMP can stabilize quickly following challenge and may be best observed in an acute treatment experiment. To better observe the metabolic shift from OXPHOS to glycolysis, the glycolytic rate assay could be employed as a rigorous method in which rapid metabolic switches can be detected (Mookerjee and Brand, 2015). In addition, determining mitochondrial mass following treatment may be another method to measure the mitochondrial response of either fission or fusion (Westermann, 2012).

While our *in vitro* results demonstrate a synergistic effect on PCa growth, the same effect was not observed in either 22Rv1-derived xenograft model (**Fig. 3**) or in the LuCaP35-CR xenograft model (**Fig. 4**). One potential reason for the significant difference between 22Rv1-derived xenograft response to combination treatment and the observable phenotype *in vitro* is the difference in the metabolic profile for 22Rv1 cells. As we observed with the MMP, 22Rv1 cells did not exhibit a difference between treatment groups, indicating that the ATP synthase remained

JPET Fast Forward. Published on October 8, 2024 as DOI: 10.1124/jpet.124.002424
This article has not been copyedited and formatted. The final version may differ from this version.

functional due to the stable polarization of the mitochondrial membrane (**Fig. 2I**). 22Rv1 cells are typically used as the standard xenograft model in testing drug-resistant CRPC as they are intrinsically resistant to enzalutamide and account for the AR-V7 (Kregel et al., 2020; Sarwar et al., 2016), however, we observed that C4-2R and MR49F cells were more sensitive to changes in metabolism than 22Rv1 cells (**Fig. 2A-H**). Another potential explanation for the difference in responses to combination treatment between *in vitro* and *in vivo* models could be the route of administration and treatment. In our study, we used an oral gavage technique with treatments at the concentrations listed in the methods section, however, utilization of an intraperitoneal technique might have yielded better results in the mice as this is a method of direct administration (Turner et al., 2011). In addition to changes in administration, metformin may be more sensitive to freeze/thaw than we anticipated. Future treatments with metformin *in vivo* may require dissolving smaller doses for treatment to avoid freeze/thawing effects. We are aware of a separate report on the combination of metformin and enzalutamide in PCa (Liu et al., 2017). In that report, the authors stated that metformin is capable of reversing enzalutamide resistance and restoring sensitivity of 22RV1 xenografts to enzalutamide (Liu et al., 2017). Accordingly, we carefully compared the experimental conditions of the two studies. In our study, we used 10 μM enzalutamide and 1 mM metformin for cell culture experiments. In the previous work, the authors used 20 μM enzalutamide and 5 mM metformin for in vitro experiments. Thus, the metformin concentration in the previous study was 5 times higher than in our study. In vivo, we used 30 mg/kg enzalutamide and 20 mg/kg metformin, whereas the previous report used 25 mg/kg enzalutamide and 300 mg/kg metformin. The metformin dose used in the previous in vivo study was 15 times higher than in our study. Because of the very high concentration of metformin used, metformin alone was sufficient to completely inhibit tumor growth, and the combination of

metformin and enzalutamide did not show a statistically significant difference compared to metformin alone (see Fig. 1e of previous study) (Liu et al., 2017). In conclusion, the 15-fold higher concentration of metformin used in the previous in vivo study is likely the main reason for the apparent discrepancy.

We acknowledge that multiple factors may affect the outcome of in vivo experiments. For example, we started the treatment when tumors reached a size of 200 mm^3, which may have been too late for optimal treatment. Early intervention could yield different results. Additionally, drug doses (as discussed above), treatment time points, and duration may also impact the outcomes of our in vivo experiments. However, we have carefully followed the well-established lab protocol, as previously published (Liu et al., 2023). Furthermore, a bone metastatic model might be a better choice for testing the effectiveness of the combination, especially given that the osteoclast differentiation genes were shown to be down-regulated (Fig. 5C). Future experiments will be designed to directly test this possibility.

RNA sequencing analysis identified an upregulation of both cell cycle and DNA repair pathways following metformin and enzalutamide treatment in enzalutamide-resistant cells (Fig. 5C, 5E). These findings suggest potential new treatment strategies, as they indicate that enzalutamide-resistant PCa cells may rely on the activation of cell cycle or DNA repair pathways to survive metformin treatment. Cell cycle regulators such as polo-like kinase 1 (Plk1) and cyclin-dependent kinases (CDKs), as well as DNA repair regulators like ATR, play well-established roles in cancer progression (Kase et al., 2020). For instance, the CDK4 inhibitor palbociclicdkb (Ibrance), which is approved for cancer treatment, is primarily used for hormone receptor-positive, HER2-negative breast cancer. Other CDK4/6 inhibitors, such as ribociclib and abemaciclib, are used in similar contexts. Several DNA damage repair inhibitors have also been approved for cancer

JPET Fast Forward. Published on October 8, 2024 as DOI: 10.1124/jpet.124.002424
This article has not been copyedited and formatted. The final version may differ from this version.

treatment. Notable examples of Poly (ADP-ribose) polymerase (PARP) inhibitors include olaparib (Lynparza), rucaparib (Rubraca), niraparib (Zejula), and talazoparib (Talzenna) (Taylor et al., 2023). While palbociclib is primarily used in breast cancer, it is currently being investigated for PCa, particularly in combination with other therapies. Further experiments are needed to determine whether metformin can enhance the efficacy of palbociclib in treating CRPC (Kase et al., 2020). Regarding DNA damage repair inhibitors, olaparib has been approved for use in PCa with BRCA1 or BRCA2 mutations and is used in patients with metastatic CRPC who have been previously treated with other therapies (Taylor et al., 2023). It would be of great interest to test whether combining metformin with olaparib could enhance efficacy in CRPC patients. Additionally, rucaparib, another PARP inhibitor being explored for prostate cancer, is particularly relevant for those with BRCA mutations. Several inhibitors targeting ATM and ATR are currently in clinical trials for prostate cancer, investigating their efficacy either alone or in combination with other therapies. In the future, we will explore whether co-administration of metformin can enhance the efficacy of these various inhibitors in treating CRPC that no longer responds to enzalutamide.

In summary, the present study demonstrates the difficulty in treating drug resistant CRPC as the combination treatment of enzalutamide and metformin *in vitro* demonstrated a positive attenuation of PCa growth, however, this effect was not observed *in vivo*. Our results highlight the importance of investigating different treatment in robust *in vitro* and *in vivo* models. Despite drug-resistant CRPC's reliance on OXPHOS in energy metabolism, inhibition of OXPHOS with metformin did not produce an observable phenotype on ENZ-r lines.

Acknowledgements:

We would like to express our sincere gratitude to Drs. Kandy Zhang, Yanquan Zhang, Jinghui Liu, and the other members of the Liu lab for their invaluable guidance and assistance in completing this project. The study was also supported by the Biospecimen Procurement & Translational Pathology, Biostatistics and Bioinformatic Shared Resources of the University of Kentucky Markey Cancer Center.

Data Availability Statement:

All data/datasets are contained in the paper.

Authorship Contribution:

Participated in research design: Simpson, J. Liu, and X. Liu

Conducted experiments: Simpson

Performed data analysis: Simpson, Allison, He, J. Liu, Wang, and X. Liu

Wrote or contributed to the writing of the manuscript: Simpson, He, and X. Liu

JPET Fast Forward. Published on October 8, 2024 as DOI: 10.1124/jpet.124.002424
This article has not been copyedited and formatted. The final version may differ from this version.

References cited:

Amaral, T.M., Macedo, D., Fernandes, I., and Costa, L. (2012). Castration-resistant prostate cancer: mechanisms, targets, and treatment. Prostate Cancer *2012*, 327253.
Antonarakis, E.S., Lu, C., Wang, H., Luber, B., Nakazawa, M., Roeser, J.C., Chen, Y., Mohammad, T.A., Chen, Y., Fedor, H.L.*, et al.* (2014). AR-V7 and resistance to enzalutamide and abiraterone in prostate cancer. N Engl J Med *371*, 1028-1038.
Bai, Y., Zhang, Z., Cheng, L., Wang, R., Chen, X., Kong, Y., Feng, F., Ahmad, N., Li, L., and Liu, X. (2019). Inhibition of enhancer of zeste homolog 2 (EZH2) overcomes enzalutamide resistance in castration-resistant prostate cancer. J Biol Chem *294*, 9911-9923.
Ben Sahra, I., Laurent, K., Loubat, A., Giorgetti-Peraldi, S., Colosetti, P., Auberger, P., Tanti, J.F., Le Marchand-Brustel, Y., and Bost, F. (2008). The antidiabetic drug metformin exerts an antitumoral effect in vitro and in vivo through a decrease of cyclin D1 level. Oncogene *27*, 3576-3586.
Berenbaum, M.C. (1989). What is synergy? Pharmacol Rev *41*, 93-141.
Chandrasekar, T., Yang, J.C., Gao, A.C., and Evans, C.P. (2015). Mechanisms of resistance in castration-resistant prostate cancer (CRPC). Transl Androl Urol *4*, 365-380.
Chen, L., Ahmad, N., and Liu, X. (2016). Combining p53 stabilizers with metformin induces synergistic apoptosis through regulation of energy metabolism in castration-resistant prostate cancer. Cell Cycle *15*, 840-849.
Cutruzzola, F., Giardina, G., Marani, M., Macone, A., Paiardini, A., Rinaldo, S., and Paone, A. (2017). Glucose Metabolism in the Progression of Prostate Cancer. Front Physiol *8*, 97.
Edlind, M.P., and Hsieh, A.C. (2014). PI3K-AKT-mTOR signaling in prostate cancer progression and androgen deprivation therapy resistance. Asian J Androl *16*, 378-386.
Efstathiou, E., Titus, M., Wen, S., Hoang, A., Karlou, M., Ashe, R., Tu, S.M., Aparicio, A., Troncoso, P., Mohler, J.*, et al.* (2015). Molecular characterization of enzalutamide-treated bone metastatic castration-resistant prostate cancer. Eur Urol *67*, 53-60.
Farah, E., Zhang, Z., Utturkar, S.M., Liu, J., Ratliff, T.L., and Liu, X. (2022). Targeting DNMTs to Overcome Enzalutamide Resistance in Prostate Cancer. Mol Cancer Ther *21*, 193-205.
Ferrick, D.A., Neilson, A., and Beeson, C. (2008). Advances in measuring cellular bioenergetics using extracellular flux. Drug Discov Today *13*, 268-274.
Horan, M.P., Pichaud, N., and Ballard, J.W. (2012). Review: quantifying mitochondrial dysfunction in complex diseases of aging. J Gerontol A Biol Sci Med Sci *67*, 1022-1035.
Kase, A.M., Copland Iii, J.A., and Tan, W. (2020). Novel Therapeutic Strategies for CDK4/6 Inhibitors in Metastatic Castrate-Resistant Prostate Cancer. Onco Targets Ther *13*, 10499-10513.
Kasznicki, J., Sliwinska, A., and Drzewoski, J. (2014). Metformin in cancer prevention and therapy. Ann Transl Med *2*, 57.
Kong, Y., Zhang, Y., Mao, F., Zhang, Z., Li, Z., Wang, R., Liu, J., and Liu, X. (2020). Inhibition of EZH2 Enhances the Antitumor Efficacy of Metformin in Prostate Cancer. Mol Cancer Ther *19*, 2490-2501.
Kregel, S., Wang, C., Han, X., Xiao, L., Fernandez-Salas, E., Bawa, P., McCollum, B.L., Wilder-Romans, K., Apel, I.J., Cao, X.*, et al.* (2020). Androgen receptor degraders overcome common resistance mechanisms developed during prostate cancer treatment. Neoplasia *22*, 111-119.
Li, C., Liu, J., He, D., Mao, F., Rao, X., Zhao, Y., Lanman, N.A., Kazemian, M., Farah, E., Liu, J.*, et al.* (2022). GSTM2 is a key molecular determinant of resistance to SG-ARIs. Oncogene *41*, 4498-4511.

Liu, J., Zhao, Y., He, D., Jones, K.M., Tang, S., Allison, D.B., Zhang, Y., Chen, J., Zhang, Q., Wang, X.*, et al.* (2023). A kinome-wide CRISPR screen identifies CK1alpha as a target to overcome enzalutamide resistance of prostate cancer. Cell Rep Med *4*, 101015.
Liu, Q., Tong, D., Liu, G., Xu, J., Do, K., Geary, K., Zhang, D., Zhang, J., Zhang, Y., Li, Y.*, et al.* (2017). Metformin reverses prostate cancer resistance to enzalutamide by targeting TGF-beta1/STAT3 axis-regulated EMT. Cell Death Dis *8*, e3007.
Mookerjee, S.A., and Brand, M.D. (2015). Measurement and Analysis of Extracellular Acid Production to Determine Glycolytic Rate. J Vis Exp, e53464.
Murtola, T.J., Tammela, T.L., Lahtela, J., and Auvinen, A. (2008). Antidiabetic medication and prostate cancer risk: a population-based case-control study. Am J Epidemiol *168*, 925-931.
Rodriguez-Berriguete, G., Fraile, B., Martinez-Onsurbe, P., Olmedilla, G., Paniagua, R., and Royuela, M. (2012). MAP Kinases and Prostate Cancer. J Signal Transduct *2012*, 169170.
Rothermundt, C., Hayoz, S., Templeton, A.J., Winterhalder, R., Strebel, R.T., Bartschi, D., Pollak, M., Lui, L., Endt, K., Schiess, R.*, et al.* (2014). Metformin in chemotherapy-naive castration-resistant prostate cancer: a multicenter phase 2 trial (SAKK 08/09). Eur Urol *66*, 468-474.
Sarwar, M., Semenas, J., Miftakhova, R., Simoulis, A., Robinson, B., Gjorloff Wingren, A., Mongan, N.P., Heery, D.M., Johnsson, H., Abrahamsson, P.A.*, et al.* (2016). Targeted suppression of AR-V7 using PIP5K1alpha inhibitor overcomes enzalutamide resistance in prostate cancer cells. Oncotarget *7*, 63065-63081.
Seruga, B., Ocana, A., and Tannock, I.F. (2011). Drug resistance in metastatic castration-resistant prostate cancer. Nat Rev Clin Oncol *8*, 12-23.
Shao, C., Ahmad, N., Hodges, K., Kuang, S., Ratliff, T., and Liu, X. (2015). Inhibition of polo-like kinase 1 (Plk1) enhances the antineoplastic activity of metformin in prostate cancer. J Biol Chem *290*, 2024-2033.
Sharifi, N., Gulley, J.L., and Dahut, W.L. (2005). Androgen deprivation therapy for prostate cancer. JAMA *294*, 238-244.
Shoag, J.E., Nyame, Y.A., Gulati, R., Etzioni, R., and Hu, J.C. (2020). Reconsidering the Trade-offs of Prostate Cancer Screening. N Engl J Med *382*, 2465-2468.
Shorning, B.Y., Dass, M.S., Smalley, M.J., and Pearson, H.B. (2020). The PI3K-AKT-mTOR Pathway and Prostate Cancer: At the Crossroads of AR, MAPK, and WNT Signaling. Int J Mol Sci *21*.
Siegel, R.L., Giaquinto, A.N., and Jemal, A. (2024). Cancer statistics, 2024. CA Cancer J Clin *74*, 12-49.
Sleire, L., Forde, H.E., Netland, I.A., Leiss, L., Skeie, B.S., and Enger, P.O. (2017). Drug repurposing in cancer. Pharmacol Res *124*, 74-91.
Sobhani, N., Neeli, P.K., D'Angelo, A., Pittacolo, M., Sirico, M., Galli, I.C., Roviello, G., and Nesi, G. (2021). AR-V7 in Metastatic Prostate Cancer: A Strategy beyond Redemption. Int J Mol Sci *22*.
Spratt, D.E., Zhang, C., Zumsteg, Z.S., Pei, X., Zhang, Z., and Zelefsky, M.J. (2013). Metformin and prostate cancer: reduced development of castration-resistant disease and prostate cancer mortality. Eur Urol *63*, 709-716.
Sukumar, M., Liu, J., Mehta, G.U., Patel, S.J., Roychoudhuri, R., Crompton, J.G., Klebanoff, C.A., Ji, Y., Li, P., Yu, Z.*, et al.* (2016). Mitochondrial Membrane Potential Identifies Cells with Enhanced Stemness for Cellular Therapy. Cell Metab *23*, 63-76.

Taylor, A.K., Kosoff, D., Emamekhoo, H., Lang, J.M., and Kyriakopoulos, C.E. (2023). PARP inhibitors in metastatic prostate cancer. Front Oncol *13*, 1159557.
Turner, P.V., Brabb, T., Pekow, C., and Vasbinder, M.A. (2011). Administration of substances to laboratory animals: routes of administration and factors to consider. J Am Assoc Lab Anim Sci *50*, 600-613.
van Soest, R.J., de Morree, E.S., Kweldam, C.F., de Ridder, C.M.A., Wiemer, E.A.C., Mathijssen, R.H.J., de Wit, R., and van Weerden, W.M. (2015). Targeting the Androgen Receptor Confers In Vivo Cross-resistance Between Enzalutamide and Docetaxel, But Not Cabazitaxel, in Castration-resistant Prostate Cancer. Eur Urol *67*, 981-985.
Wang, Y., Chen, J., Wu, Z., Ding, W., Gao, S., Gao, Y., and Xu, C. (2021). Mechanisms of enzalutamide resistance in castration-resistant prostate cancer and therapeutic strategies to overcome it. Br J Pharmacol *178*, 239-261.
Weber, M.J., and Gioeli, D. (2004). Ras signaling in prostate cancer progression. J Cell Biochem *91*, 13-25.
Westermann, B. (2012). Bioenergetic role of mitochondrial fusion and fission. Biochim Biophys Acta *1817*, 1833-1838.
Zhao, Y., Zeng, X., Tang, H., Ye, D., and Liu, J. (2019). Combination of metformin and paclitaxel suppresses proliferation and induces apoptosis of human prostate cancer cells via oxidative stress and targeting the mitochondria-dependent pathway. Oncol Lett *17*, 4277-4284.

Footnotes:

This work was supported by the National Institutes of Health National Cancer Institute [R01 CA256893, R01 CA264652, R01 CA157429, R01 CA272483, P30 CA177558]. No author has an actual or perceived conflict of interest with the contents of this article.

JPET Fast Forward. Published on October 8, 2024 as DOI: 10.1124/jpet.124.002424
This article has not been copyedited and formatted. The final version may differ from this version.

Figure Legends:

Figure 1: Enzalutamide and Metformin in combination synergistically inhibit growth of enzalutamide resistant CRPC *in vitro*.

Cell viability assay of isogenic CRPC lines treated with either enzalutamide **(A, C, E)** or metformin **(B, D, F)** to compare IC_{50} values. Data is scaled into percentage and normalized to untreated groups, then shown as mean ±SD (n=3). Clonogenic assay of MR49F **(G)**, C4-2R **(H)**, and 22Rv1 **(I)** treated with DMSO as control or drugs indicated for up to 14 days. Quantification of relative colony number are indicated below where *, $p \leq 0.05$; **, $p \leq 0.01$; ***, $p \leq 0.001$. Synergy scores were calculated for 22Rv1 **(J)**, C4-2R **(K)**, and MR49F **(L)** after treatment with varying doses of the indicated drugs. Scores ≤ -10 indicate an antagonistic interaction, scores between -10 and 10 indicate an additive effect, and scores ≥ 10 are considered synergistic.

Figure 2: Combination treatment results in metabolic reprograming.

Representative traces of the oxygen consumption rate (OCR), when oligomycin, carbonyl cyanide-4-(trifluoromethoxy) phenylhydrazone (FCCP), antimycin A plus rotenone were injected into the assay XF96 plates for MR49F **(A-C)** and C4-2R **(D-F)** cells. Each data point is a mean ± standard deviation (n=6). Cells were treated with or without 10μM enzalutamide, 1mM metformin, or a combination of both for 12 hours. Mitochondrial membrane potential was measured using tetramethylrhodamine, ethyl ester, perchlorate (TMRE). MR49F **(G)**, C4-2R **(H)**, and 22Rv1 **(I)** cells were treated with or without enzalutamide, metformin, or a combination of both for 12 hours and collected for flow cytometric analysis. FCCP was used as a positive control. **(J)** The mitochondrial membrane potential was measured with the same treatment as with TMRE in all 3 resistant lines, but the chemical JC-1 was used to visualize the membrane potential shift.

JPET Fast Forward. Published on October 8, 2024 as DOI: 10.1124/jpet.124.002424
This article has not been copyedited and formatted. The final version may differ from this version.

Figure 3: Combination treatment of enzalutamide and metformin did not attenuate 22Rv1 Xenograft tumor growth *in vivo*.

(A) Tumor growth curves of 22Rv1-derived xenograft. After pre-castrated nude mice were inoculated subcutaneously with 22Rv1 cells ($2.5X10^6$/mouse) and allowed to grow for 2 weeks. After 2 weeks, the mice were treated with various drugs as described in the methods section of this chapter. The sizes of the tumors in each group were measured every 3 days (mean ± SD; n= 13 mice per group). **(B)** Measurement of tumor weight immediately after harvest. **(C)** Images of 22Rv1-derived tumors at the end of the study. **(D)** Measurement of mouse body weight throughout the study. **(E)** Representative images of H&E staining on formaldehyde-fixed, paraffin-embedded, 22Rv1-derived tumor sections. **(F)** Representative images of anti-Ki67 IHC staining of tumor sections. **(G)** Representative images of anti-cleaved caspase-3 IHC staining of tumor sections.

Figure 4: Combination treatment of enzalutamide and metformin did not attenuate LuCaP35CR tumor growth *in vivo*.

(A) Tumor growth curves of LuCaP35CR xenografts (mean ± SD; n= 4 mice per group). **(B)** Measurement of tumor weight immediately after harvest. **(C)** Images of LuCaP35CR tumors at the end of the study. **(D)** Measurement of mouse body weight throughout the study.

Figure 5: RNA sequencing analysis of isogenic CRPC lines.

(A) Schematic representation of gene comparisons for RNA sequencing result analysis. Dot plot analysis of significant C4-2R downregulated **(B)**, upregulated **(C)**, MR49F downregulated **(D)**, and upregulated **(E)** pathways. Methods: The RNA-Seq DE analysis involved the following comparisons and cell lines: 1) Metformin vs. Control in the C4-2 cell line; 2) Metformin vs. Control in the C4-2R cell line; and 3) Combo vs. Control in the C4-2R cell line. Additionally, three more comparisons were performed in parallel with the above three: 4) Metformin vs. Control in

JPET Fast Forward. Published on October 8, 2024 as DOI: 10.1124/jpet.124.002424
This article has not been copyedited and formatted. The final version may differ from this version.

the LNCaP cell line; 5) Metformin vs. Control in the MR49F cell line; and 6) Combo vs. Control in the MR49F cell line. In this setup, the LNCaP cell line serves as a parallel to the C4-2 cell line, and the MR49F cell line serves as a parallel to the C4-2R cell line. For each comparison, RNA-Seq DE analysis was conducted using the R package "edgeR," with the control group chosen as the reference. In comparisons 1-3 and 4-6, respectively, significantly up-regulated DE genes were identified by a log2(fold change) > 0.5 and a q-value < 0.05, while significantly down-regulated DE genes were identified by a log2(fold change) < -0.5 and a q-value < 0.05. We then isolated the significant DE genes that were found in the combo vs. control comparison but not in the metformin vs. control comparison, identifying genes that responded exclusively to the combo treatment. Using this subset of up-regulated or down-regulated DE genes, we performed KEGG pathway enrichment analysis with the R package "clusterProfiler," which uses Fisher's exact test. The output of the enrichment analysis reveals the KEGG pathways that are enriched specifically in response to the combo treatment. Figure 5 illustrates the top 20 up-regulated and down-regulated KEGG pathways with the smallest p-values for the cell lines C4-2/C4-2R and LNCaP/MR49F, respectively.

JPET Fast Forward. Published on October 8, 2024 as DOI: 10.1124/jpet.124.002424

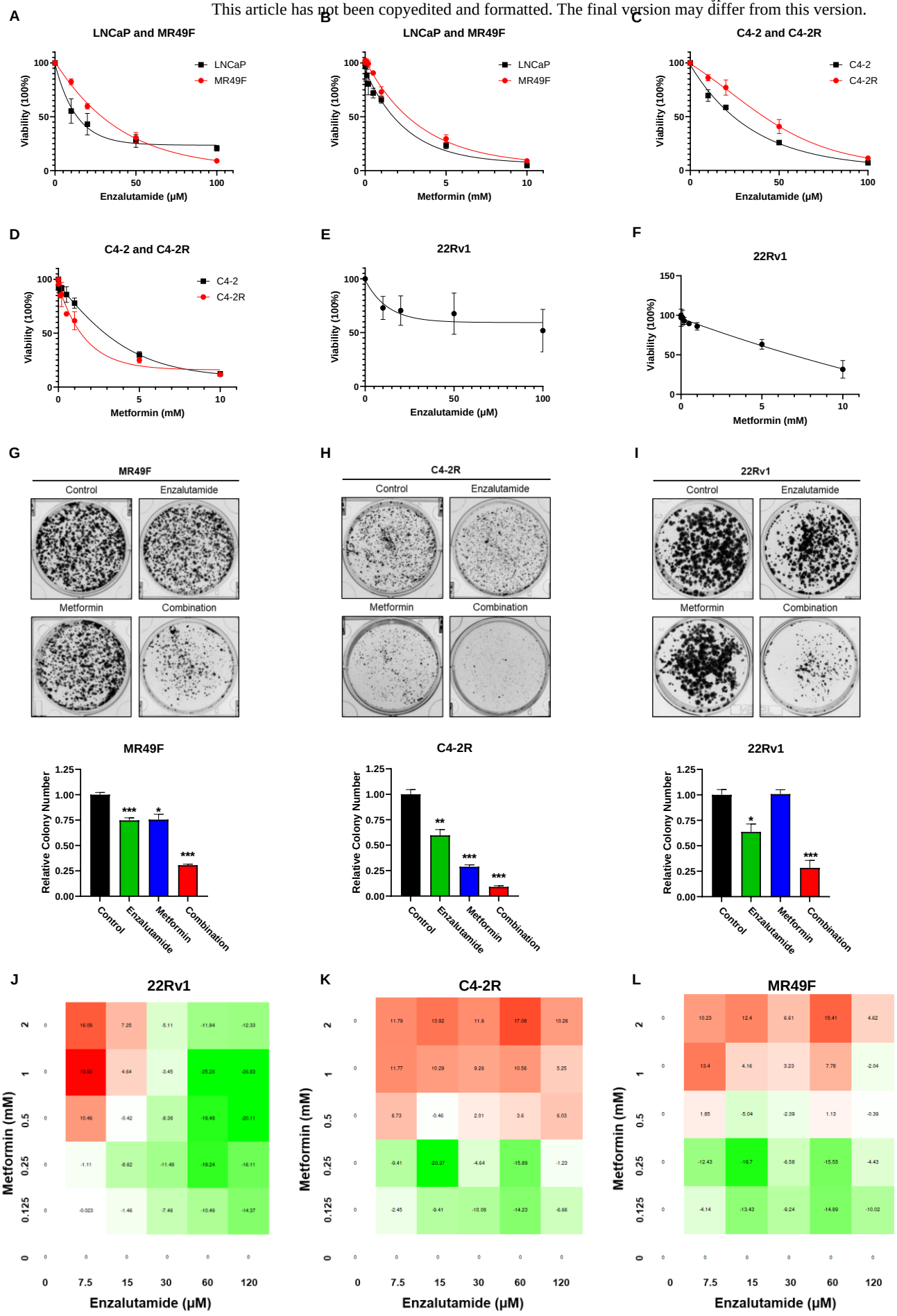

Figure 1

JPET Fast Forward. Published on October 8, 2024 as DOI: 10.1124/jpet.124.002424

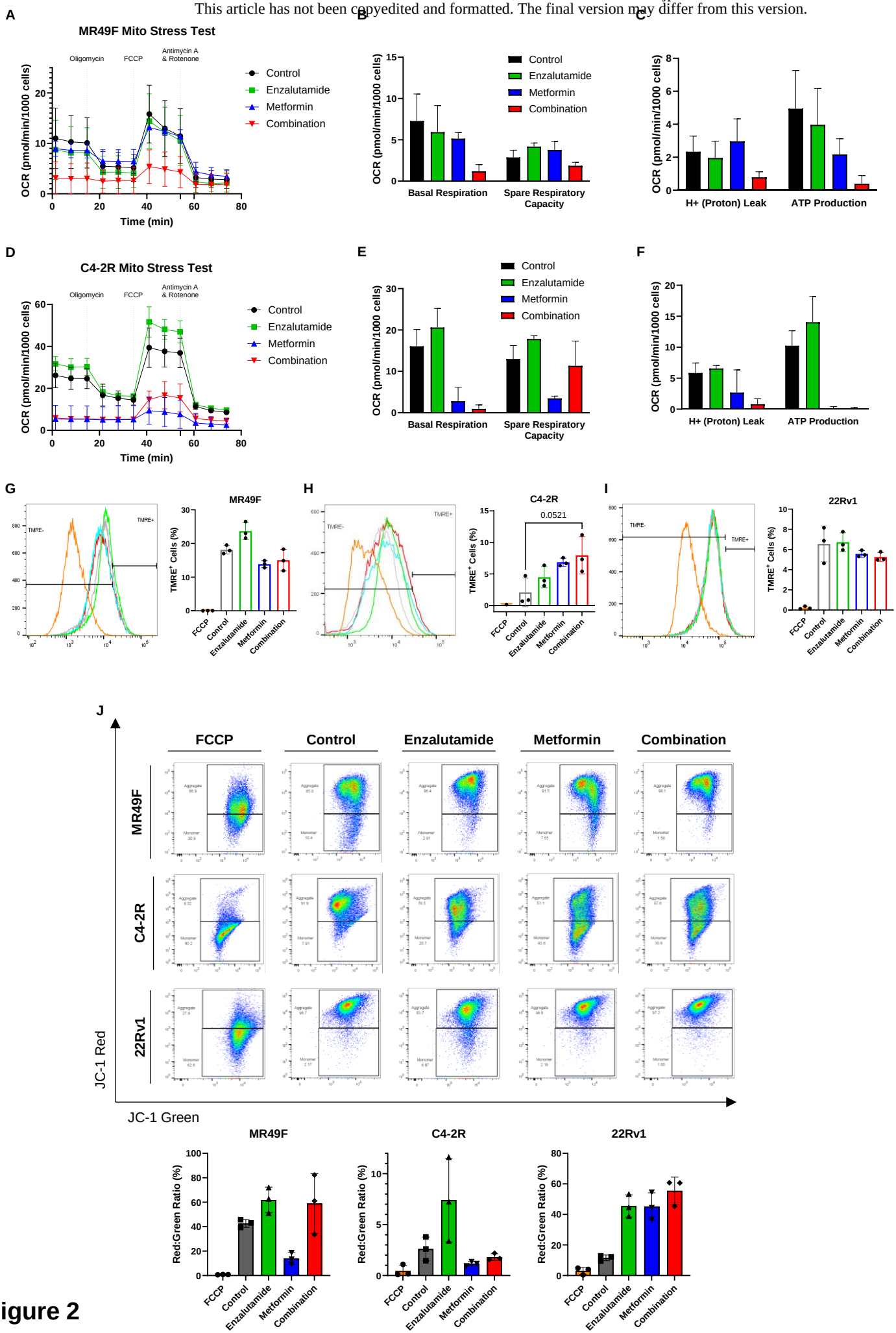

Figure 2

JPET Fast Forward. Published on October 8, 2024 as DOI: 10.1124/jpet.124.002424

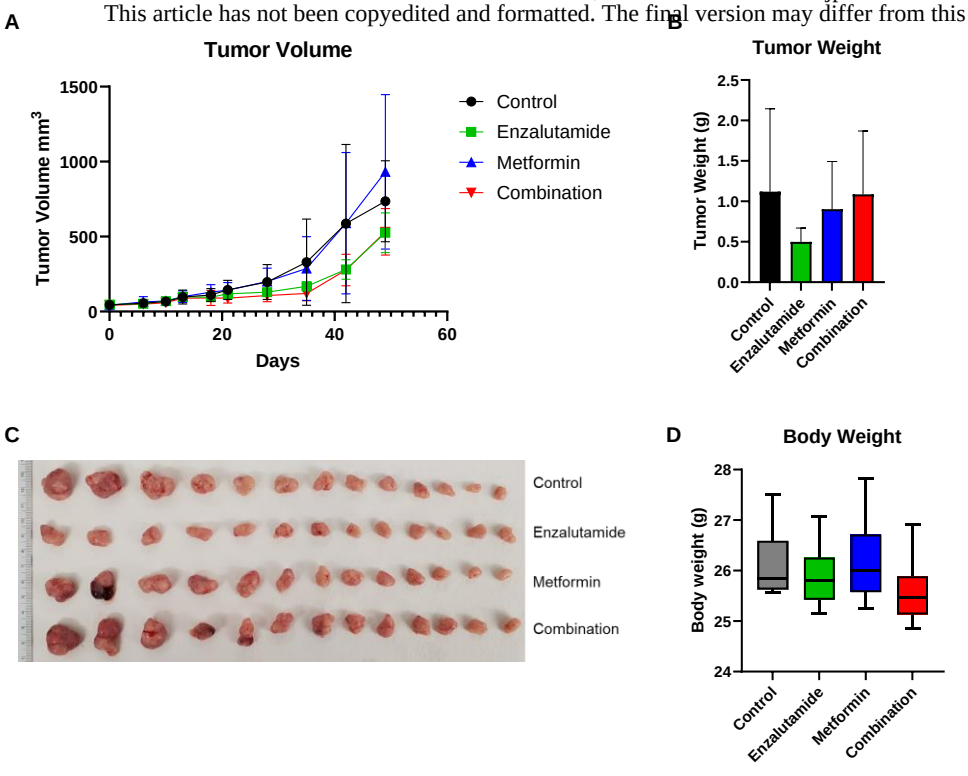

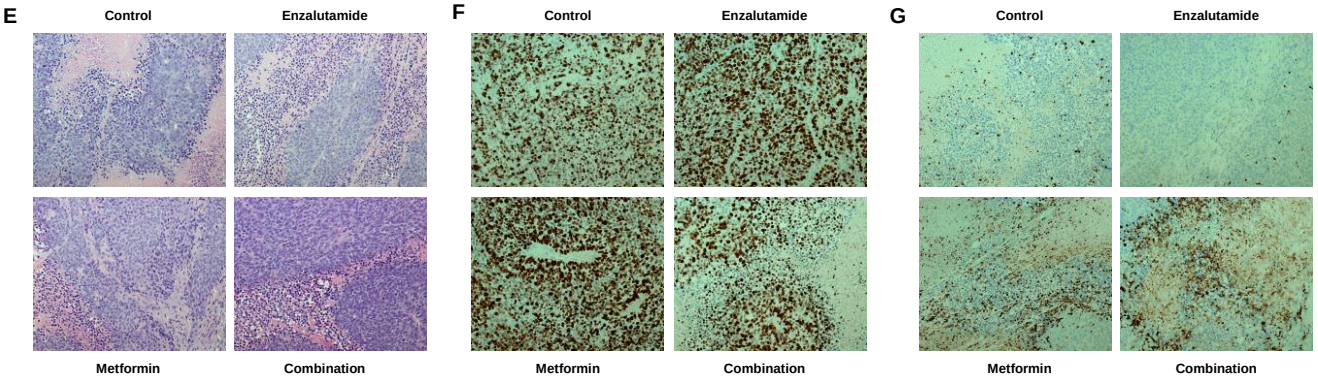

Figure 3

JPET Fast Forward. Published on October 8, 2024 as DOI: 10.1124/jpet.124.002424

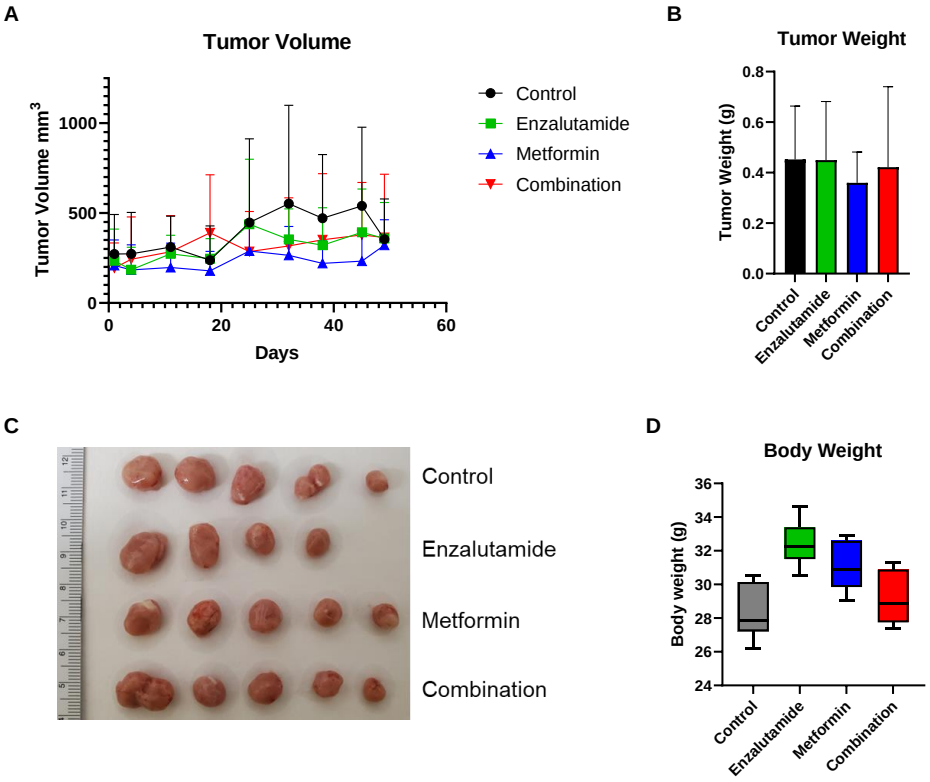

Figure 4

JPET Fast Forward. Published on October 8, 2024 as DOI: 10.1124/jpet.124.002424

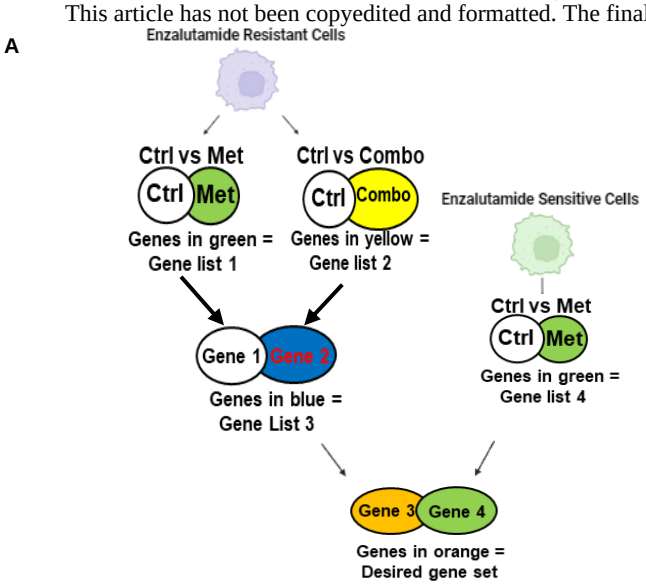

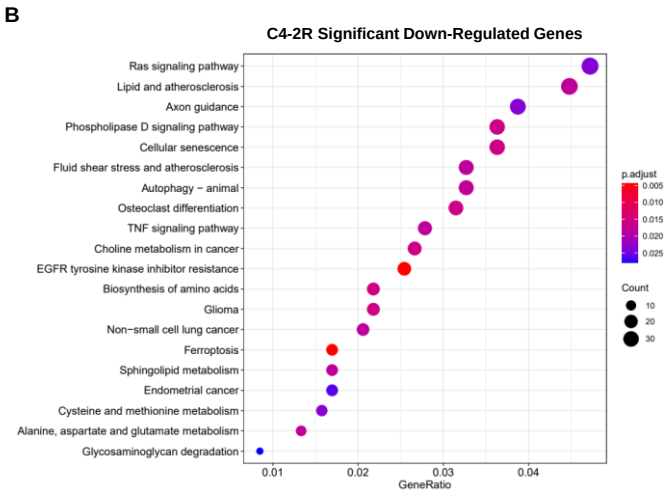

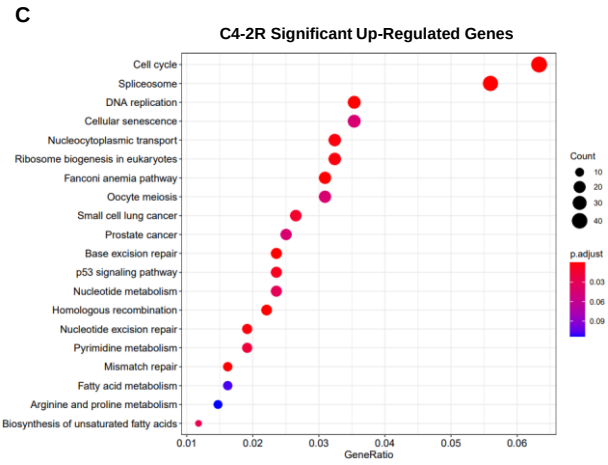

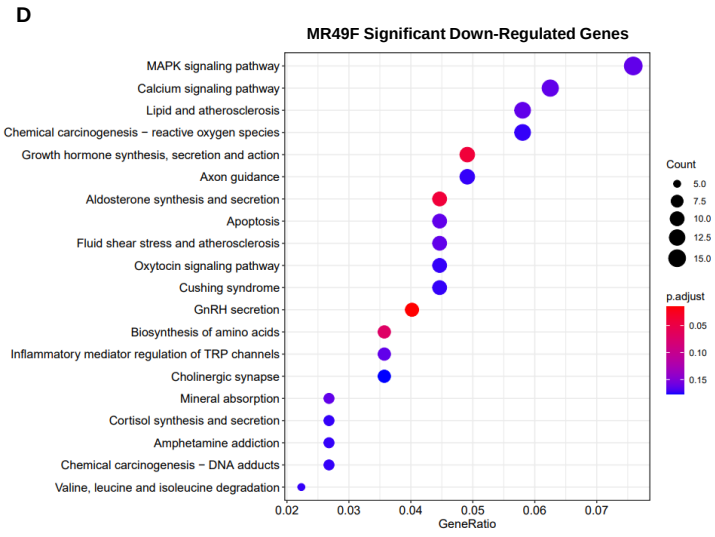

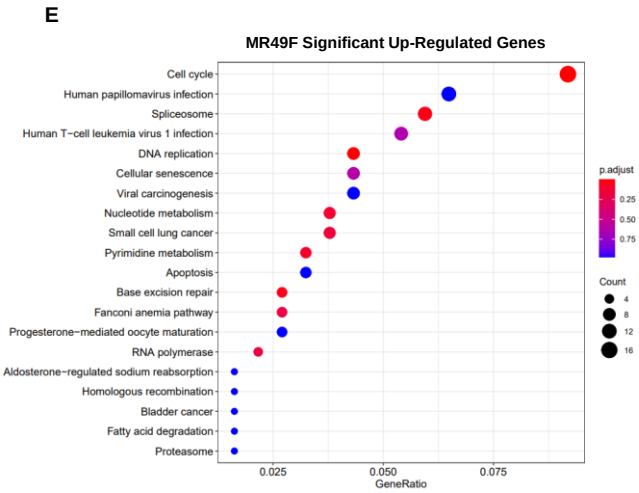

Figure 5